

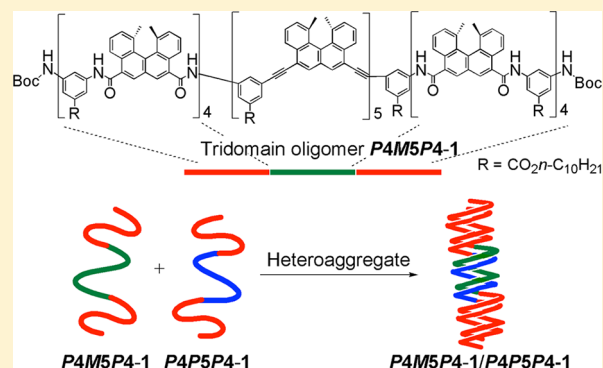
# Heteroaggregation between Isomeric Amido-ethynyl-amidohelicene Tridomain Oligomers

Wataru Ichinose, Jun Ito, and Masahiko Yamaguchi\*

Department of Organic Chemistry, Graduate School of Pharmaceutical Sciences, Tohoku University, Aoba, Sendai 980-8578, Japan

**S** Supporting Information

**ABSTRACT:** Three isomers, i.e., *P4M5P4-1*, *M4P5M4-1*, and *M4M5M4-1*, of amido-ethynyl-amidohelicene tridomain oligomers were synthesized. *P4M5P4-1* formed four homoaggregate states, i.e., all-dimer, amido-dimer, ethynyl-dimer, and random-coil states, by independent aggregation and disaggregation at the ethynyl and amido domains. Then, possible combinations of heteroaggregation were examined between the isomeric tridomain oligomers *P4P5P4-1*, *P4M5P4-1*, *M4P5M4-1*, and *M4M5M4-1*. When *P4P5P4-1* and *P4M5P4-1* were mixed in THF, to which trifluoromethylbenzene was added, heteroaggregates with an all-dimer structure were formed without forming homoaggregates. The heteroaggregation initially occurred at the central ethynyl domain, which was followed by the aggregation at the amido domains. Heteroaggregates were also formed using the combinations *P4P5P4-1*/*M4M5M4-1* and *P4M5P4-1*/*M4P5M4-1*, and the results indicated an important role for the central ethynyl domain for heteroaggregation.



## INTRODUCTION

Heteroaggregation between different structures of proteins plays important roles in biological systems.<sup>1</sup> In such cases, heteroaggregation must be much stronger than homoaggregation; otherwise, mixtures of heteroaggregates and homoaggregates will be formed. The formation of mixtures may not be desirable when a structural signal of heteroaggregation is transferred to other biological events. It is therefore interesting to understand how homoaggregation is suppressed and how heteroaggregation is promoted at the protein molecular level, because the general concept of such suppression and promotion remains unknown.

Proteins are multidomain compounds with different structures and properties at each domain, and their functions differ with their combination. It is therefore interesting to study how heteroaggregation occurs in multidomain compounds, and the examination of synthetic multidomain compounds is attractive for this purpose, because the molecular structure at each domain and their connecting mode can be designed. In addition, structure and property can be analyzed by various methods. Heteroaggregate formation of multidomain compounds has been studied using block copolymers, which provided controlled macroscopic structures. Block copolymers containing peptides,<sup>2</sup> aromatic amides,<sup>3</sup> nucleobases,<sup>4</sup> and phenols<sup>5</sup> were treated with other polymers to form micelles and separated phases, in which hydrogen bonding was employed for the heteroaggregation. Poly(ethylene glycol)-containing amphiphilic block copolymers were also used for heteroaggregation under aqueous conditions.<sup>6</sup> The heteroaggregation between enantiomeric polylactide block copolymers, stereocomplex, was reported to form gels, micelles, and microspheres.<sup>7</sup>

The multiple heteroaggregation of block copolymers provides sophisticated macroscopic structures. However, to understand protein properties and to construct a well-defined functional materials system, the study on the molecular heteroaggregation<sup>8</sup> of multidomain compounds, in particular dimeric aggregation, was considered interesting. Such study was not conducted previously because of the lack of multidomain compound with oligomeric structure exhibiting well-defined dimeric heteroaggregation.

Previously, we synthesized the tridomain compound *P4P5P4-1*<sup>9</sup> by the coupling reaction of two (*P*)-amidohelicene tetramers (*P*)-2<sup>10</sup> and one (*P*)-ethynylhelicene pentamer (*P*)-3,<sup>11</sup> both of which formed dimeric homoaggregates: *P4P5P4-1* has two amido domains at the terminus and an ethynyl domain at the center.<sup>11</sup> The homoaggregation of *P4P5P4-1* was examined, and it was found that each domain independently aggregates and disaggregates in a well-defined manner. Two types of thermal response were obtained depending on the type of solvent on the basis of well-defined structural changes in multidomain compounds. We also reported the heterodouble-helix formation of pseudoenantiomeric ethynylhelicene oligomers<sup>12</sup> and their higher assembly to form two-component gels.<sup>13</sup> The dimeric heteroaggregation was much stronger than homoaggregation in these systems.<sup>14</sup> On the basis of these results, we considered it interesting to examine heteroaggregate phenomenon using the tridomain compound *P4P5P4-1* and its stereoisomers.

Received: September 9, 2012

Published: October 30, 2012

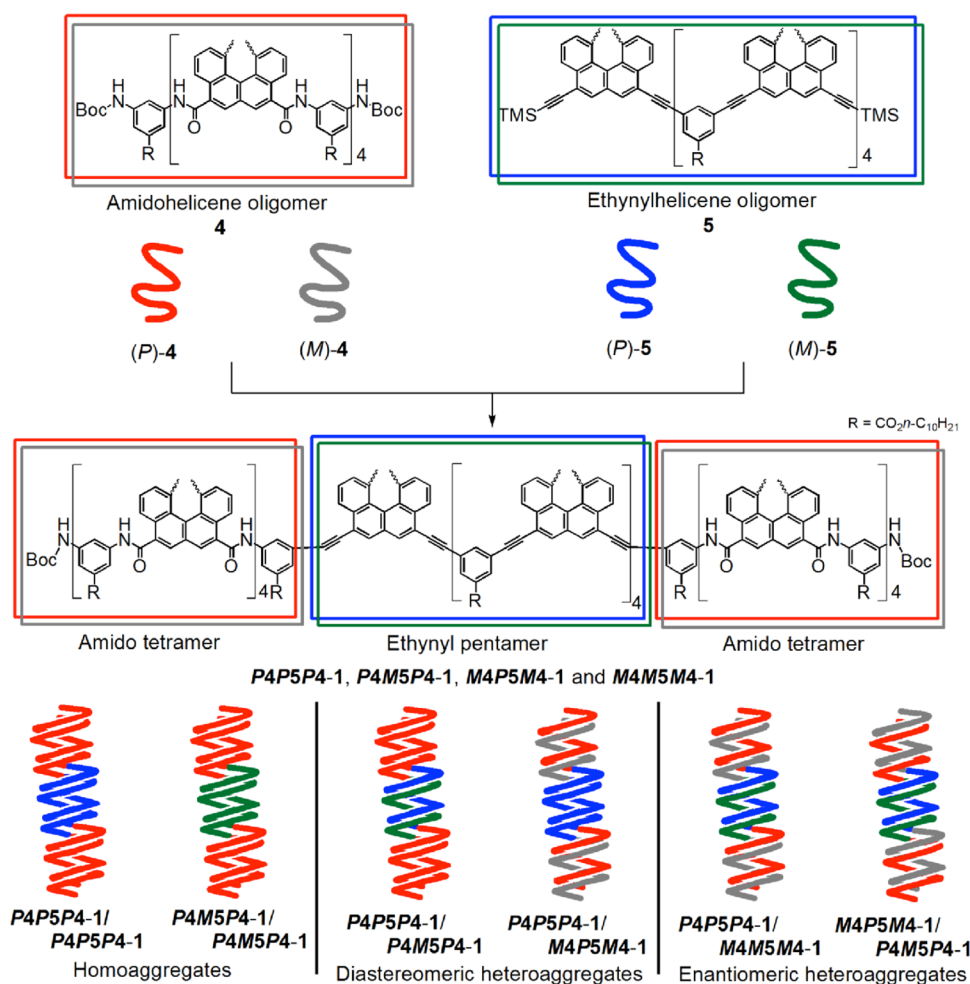
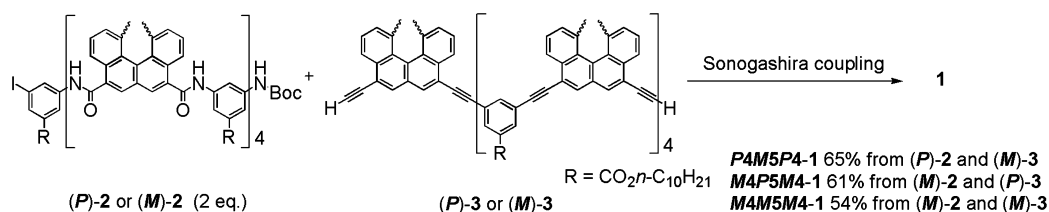


Figure 1. Six dimeric aggregates of tridomain oligomers.

### Scheme 1



In regard to the stereoisomerism of the tridomain compound **P4P5P4-1** with symmetric structure, we considered three other isomers: **P4M5P4-1**, **M4P5M4-1**, and **M4M5M4-1**. Six dimeric aggregates can then be obtained in their combinations excluding enantiomers (Figure 1). Of these aggregates, **P4P5P4-1/P4P5P4-1** and **P4M5P4-1/P4M5P4-1** are homoaggregates, **P4P5P4-1/M4M5M4-1** and **P4M5P4-1/M4P5M4-1** are racemic heteroaggregates, and **P4P5P4-1/P4M5P4-1** and **P4P5P4-1/M4P5M4-1** are diastereomeric heteroaggregates. It was considered interesting to examine heteroaggregation between stereoisomers, which was expected to promote our understanding of the heteroaggregation property of multidomain compounds.

In this study, three novel isomers, i.e., **P4M5P4-1**, **M4P5M4-1**, and **M4M5M4-1**, were synthesized, and aggregation of five combinations, i.e., **P4M5P4-1/P4M5P4-1**, **P4P5P4-1/P4M5P4-1**, **P4P5P4-1/M4P5M4-1**, **P4P5P4-1/M4M5M4-1**, and **P4M5P4-1/M4P5M4-1**, were compared with each other and

with **P4P5P4-1/P4P5P4-1**. Notably, the three combinations **P4P5P4-1/P4M5P4-1**, **P4P5P4-1/M4M5M4-1**, and **P4M5P4-1/M4P5M4-1** formed dimeric heteroaggregates without forming homoaggregates. The heteroaggregation took place via strong and initial heteroaggregation at the central ethynyl domain.

## RESULT AND DISCUSSION

### Synthesis of **P4M5P4-1**, **M4P5M4-1**, and **M4M5M4-1**.

The synthesis of the isomeric tridomain compounds **P4M5P4-1**, **M4P5M4-1**, and **M4M5M4-1** was conducted as reported previously using the coupling reaction of isomeric oligomers.<sup>9</sup> The Sonogashira coupling of (P)-2 and 2 equiv of (M)-3 gave **P4M5P4-1** in 65% yield (Scheme 1). Similarly, **M4P5M4-1** and **M4M5M4-1** were obtained in 61% and 54% yields, respectively. The stereochemistry did not largely affect the efficiency of the synthesis.

**Homoaggregation of P4MSP4-1.** The homoaggregation of P4MSP4-1 (Figure 2) was examined in solution, employing

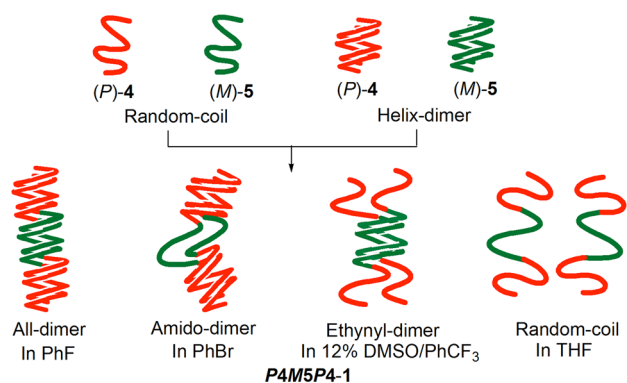


**Figure 2.** Four homoaggregate states of P4MSP4-1.

the CD method previously reported.<sup>9</sup> The CD spectra of P4MSP4-1 were compared with the calculated spectra obtained by adding those of amidohelicene tetramer 4<sup>10</sup> and ethynylhelicene pentamer 5<sup>11</sup> at the aggregate or disaggregate states: 4 was aggregated in chloroform and disaggregated in THF; 5 was aggregated in trifluoromethylbenzene and disaggregated in chloroform. Dynamic light scattering (DLS) and atomic force microscopy (AFM) analyses were conducted to confirm no higher aggregate formation and to compare the aggregate size with P4PSP4-1.<sup>9</sup> It was previously determined that a bidomain compound formed dimeric aggregate by VPO,<sup>9</sup> AFM analysis of which provided 30 nm average diameter. Then, in case similar sizes are obtained,

the formation of dimeric aggregate can reasonably be concluded for the tridomain compounds. As in the case of P4PSP4-1, four aggregate states, namely, the S-all-dimer, S-amido-dimer, S-ethynyl-dimer, and S-random-coil, were obtained by changing the solvent, in which S indicates the shifted state of equilibrium.<sup>9</sup>

The amido-dimer state of P4MSP4-1 was examined in bromobenzene as was in the case of P4PSP4-1.<sup>9</sup> The CD spectra of the aggregated amidohelicene oligomer (P)-4<sup>10</sup> (chloroform) added to the enantiomeric spectrum of the disaggregated ethynylhelicene oligomer (P)-5<sup>11a</sup> (chloroform) in 2:1 ratio was used as the calculated spectrum of the amido-dimer state of P4MSP4-1. The experimental CD spectra ( $2.5 \times 10^{-6}$  M, 25 °C) of P4MSP4-1 coincided with the calculated spectrum (Figure 3a). To confirm that this is the equilibrium shifted S-state, temperature and concentration were changed. The spectra did not change between -5 °C and 80 °C at  $2.5 \times 10^{-6}$  M (Figure 3a) or between 5 °C and 60 °C at  $2.5 \times 10^{-5}$  M (Figure 3b, and Figure S1, Supporting Information). Thus, it was concluded that P4MSP4-1 is the S-amido-dimer state under these conditions, containing no all-dimer, ethynyl-dimer, or random-coil state.

The S-all-dimer state was examined in fluorobenzene as was in the case of P4PSP4-1.<sup>9</sup> The calculated spectrum was obtained by adding the CD spectra of aggregated (P)-4<sup>10</sup> (chloroform) and the enantiomeric spectrum of aggregated (P)-5<sup>9</sup> (trifluoromethylbenzene) in 2:1 ratio. The experimental CD spectra ( $2.5 \times 10^{-6}$  M, 25 °C) of P4MSP4-1 obtained are in agreement with the calculated spectrum in shape, although the intensity decreased (Figure 4a). At 5 °C and -5 °C, the same spectrum as that at 25 °C was obtained, CD intensity decreased at 60 and 80 °C. An isosbestic point was observed at 349 nm, which is

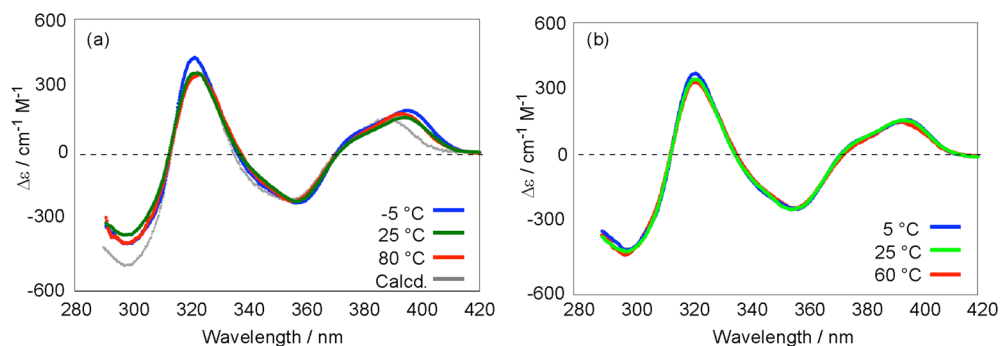


**Figure 3.** CD spectra of P4MSP4-1 in bromobenzene at different temperatures at concentrations of (a)  $2.5 \times 10^{-6}$  M and (b)  $2.5 \times 10^{-5}$  M. The calculated spectrum was obtained by adding the CD spectra of the aggregated amidohelicene oligomer (P)-4<sup>10</sup> (chloroform) and the enantiomeric spectrum of the disaggregated ethynylhelicene oligomer (P)-5<sup>11a</sup> (chloroform) in 2:1 ratio.

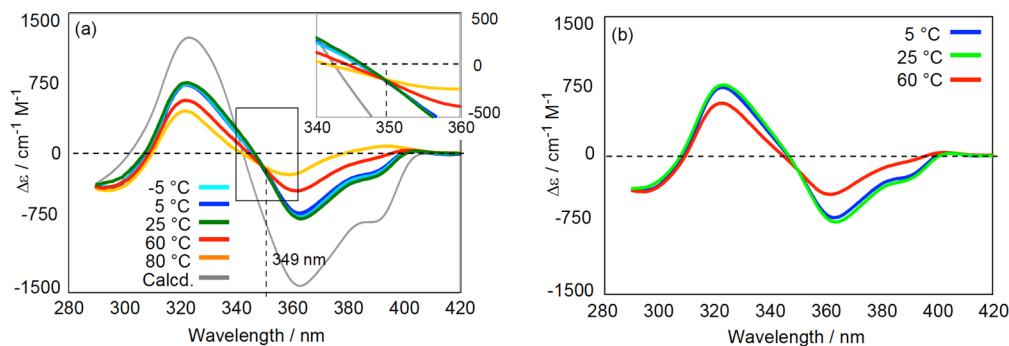


**Figure 4.** CD spectra of P4MSP4-1 in fluorobenzene at different temperatures at concentrations of (a)  $2.5 \times 10^{-6}$  M and (b)  $2.5 \times 10^{-5}$  M. The calculated spectrum was obtained by adding the CD spectra of aggregated (P)-4<sup>10</sup> (chloroform) and the enantiomeric spectrum of aggregated (P)-5<sup>9</sup> (trifluoromethylbenzene) in 2:1 ratio. The inset shows the expansion of the spectrum between 340 and 360 nm.

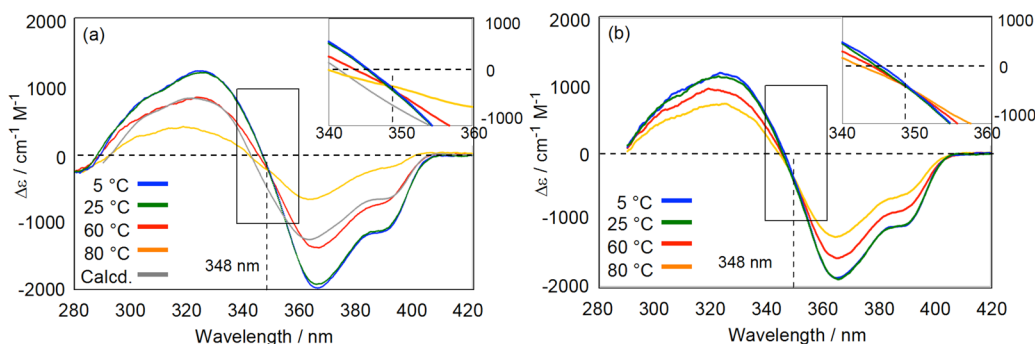


**Figure 5.** CD spectra of **P4MSP4-1** in 12% DMSO/trifluoromethylbenzene at different temperatures at concentrations of (a)  $5 \times 10^{-5}$  M and (b)  $1 \times 10^{-4}$  M. The calculated spectrum was obtained by adding the CD spectra of disaggregated (*P*-4<sup>9</sup> (THF) and the enantiomeric spectrum of aggregated (*P*-5<sup>9</sup> (trifluoromethylbenzene) in 2:1 ratio. The insets show the expansion of the spectra between 340 and 360 nm.

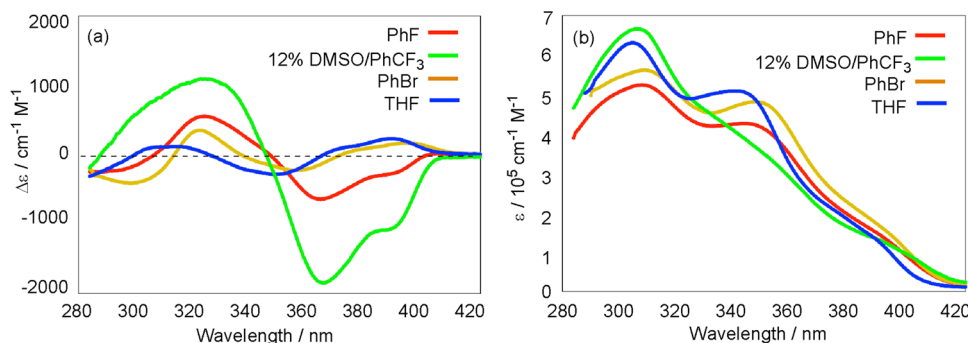


**Figure 6.** (a) CD and (b) UV–vis spectra of four aggregate S-states of **P4MSP4-1** in 12% DMSO/trifluoromethylbenzene ( $5 \times 10^{-5}$  M, 5 °C), THF, bromobenzene, and fluorobenzene ( $2.5 \times 10^{-6}$  M, 25 °C).

consistent with partial disaggregation at the ethynyl domain by the temperature change. Under the conditions, (*P*-5 was known partially to disaggregate by heating,<sup>11a</sup> whereas (*P*-4 formed strong aggregate.<sup>10</sup> At  $2.5 \times 10^{-5}$  M, the same CD spectra were obtained at 5 °C and 25 °C (Figures 4b, and Figure S2, Supporting Information). The results indicated that **P4MSP4-1** is the S-all-dimer state under these conditions.

The S-random-coil state of **P4MSP4-1** was examined in THF. The calculated spectrum was obtained by adding the CD spectra of disaggregated (*P*-4<sup>9</sup> (THF) and the enantiomeric spectrum of disaggregated (*P*-5<sup>11a</sup> (chloroform) in 2:1 ratio. The experimental CD spectra ( $2.5 \times 10^{-6}$  M, 25 °C) coincided with the calculated spectrum (Figure S3a, Supporting Information). The spectra did not change between –5 °C and 60 °C at  $2.5 \times 10^{-6}$  M (Figure S3a) or between 5 °C and 60 °C at  $2.5 \times 10^{-5}$  M (Figures S3b and S4, Supporting Information). Thus, it was concluded that **P4MSP4-1** here is the S-random-coil state.

The S-ethynyl-dimer state of **P4MSP4-1** was examined in 12% DMSO/trifluoromethylbenzene. The calculated CD spectrum was obtained by adding that of disaggregated (*P*-4<sup>9</sup> (THF) and the enantiomeric spectrum of aggregated (*P*-5<sup>9</sup> (trifluoromethylbenzene) in 2:1 ratio. The experimental CD spectra ( $5 \times 10^{-5}$  M, 5 °C) are in agreement with the calculated spectrum, except for a slight decrease in intensity (Figure 5a). The spectrum did not change at 25 °C at the same concentration. The decrease in intensity at 60 °C and 80 °C was observed with an isosbestic point at 348 nm, which is again consistent with partial disaggregation at the ethynyl domain. As for the effect of concentration at 5 °C, no change was observed at  $1 \times 10^{-4}$  M compared with that at  $5 \times 10^{-5}$  M (Figure 5b), but the Cotton effect was slightly suppressed at  $2.5 \times 10^{-5}$  M (Figure S5, Supporting Information).

It was considered that **P4MSP4-1** was the S-ethynyl-dimer state at concentrations higher than  $5 \times 10^{-5}$  M and at the temperature of 5 °C.

Four S-states of **P4MSP4-1** were obtained in solution by changing the solvent, and different CD and UV–vis spectra were obtained (Figure 6).

DLS analysis of the four states of **P4MSP4-1** was conducted (Figure 7). The amido-dimer state in bromobenzene ( $5 \times 10^{-5}$  M,

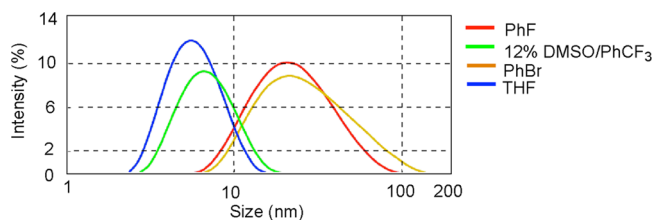


**Figure 7.** Size distributions of **P4MSP4-1** determined by DLS experiments in different solvents ( $5 \times 10^{-5}$  M, 20 °C).

20 °C) and the all-dimer state in fluorobenzene ( $5 \times 10^{-5}$  M, 20 °C) were approximately 25 nm in diameter, whereas the random-coil state in THF ( $5 \times 10^{-5}$  M, 20 °C) and the ethynyl-dimer state in 12% DMSO/trifluoromethylbenzene ( $5 \times 10^{-5}$  M, 20 °C) had an average diameter range of 6–8 nm. Similar results on the aggregate sizes were obtained for **P4PSP4-1**<sup>9</sup> previously described, and it was concluded that the homoaggregates of **P4MSP4-1** are dimeric.

The thermal structural changes of **P4MSP4-1** during the aggregation and disaggregation at the central ethynyl domain were examined using the CD spectra of the S-states (Figure 8).



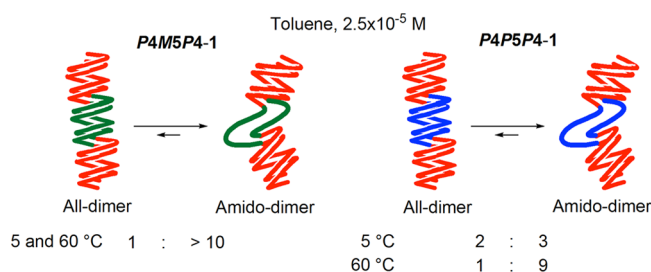


**Figure 8.** Thermal structural changes between all-dimer and amido-dimer.

When **P4M5P4-1** was dissolved in toluene ( $2.5 \times 10^{-5}$  M) and warmed at 60 °C, the S-amido-dimer state was obtained as indicated by CD spectra (Figure 9). The spectra at 5 °C were

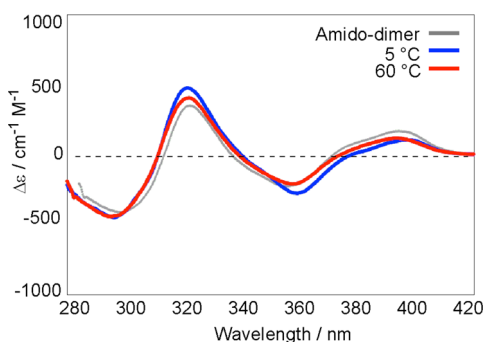


**Figure 9.** CD spectra of **P4M5P4-1** in toluene ( $2.5 \times 10^{-5}$  M) at 5 and 60 °C. The spectrum of the S-amido-dimer (Figure 6a, bromobenzene) is also shown.

essentially the same at 60 °C. The thermal stabilities of **P4M5P4-1** and **P4P5P4-1** all-dimer aggregates were compared under the same conditions. **P4P5P4-1** was a 2:3 mixture of the all-dimer and amido-dimer at 5 °C and a 1:9 mixture at 60 °C (Figure S6, Supporting Information).

The heating experiment was also conducted for **P4M5P4-1** in 12% DMSO/trifluoromethylbenzene to compare the ethynyl-dimer aggregates of **P4P5P4-1** (Figure 10). **P4M5P4-1** was a

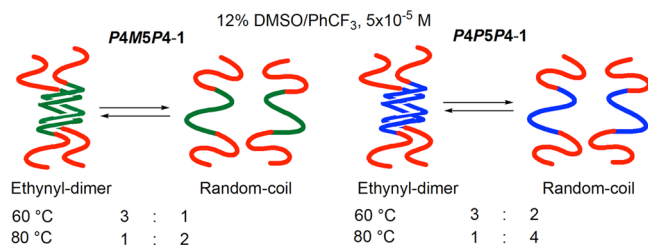


**Figure 10.** Thermal structural changes between ethynyl-dimer and random-coil.

3:1 mixture of the ethynyl-dimer and random-coil at 60 °C and a 1:2 mixture at 80 °C (Figure 11). The calculated CD spectra were obtained by adding those of the S-ethynyl-dimer (Figure 6a, 12% DMSO/trifluoromethylbenzene) and S-random-coil (Figure 6a, THF) of **P4M5P4-1** in a 3:1 ratio and in a 1:2 ratio, which were in good agreement with the experimental spectra at 60 °C and at 80 °C, respectively. To compare, **P4P5P4-1** was a 3:2 mixture of the ethynyl-dimer and random-coil at 60 °C and a 1:4 mixture at 80 °C (Figure S7, Supporting Information). Relatively small effects of stereochemistry on the thermal

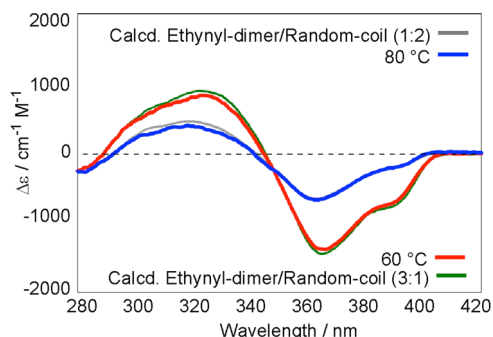


**Figure 11.** CD spectra of **P4M5P4-1** in 12% DMSO/trifluoromethylbenzene ( $5 \times 10^{-5}$  M) at 60 °C and 80 °C. The experimental spectra (blue and red line) were taken from Figure 5a. The calculated spectrum for the 3:1 state (green line) was obtained by adding the spectra of 3/4 of the S-ethynyl-dimer state (Figure 6a, 12% DMSO/trifluoromethylbenzene) and 1/4 of the S-random-coil state (Figure 6a, THF). The calculated spectrum for the 1:2 state (gray line) was obtained by adding the spectra of 1/3 of the S-ethynyl-dimer state and 2/3 of the S-random-coil state.

properties of **P4M5P4-1** and **P4P5P4-1** in the aggregation and disaggregation at the central ethynyl domain were observed, although the **P4P5P4-1** all-dimer aggregate was slightly more stable than the **P4M5P4-1** all-dimer aggregate.

The multidomain compound **P4M5P4-1** exhibited similar homoaggregation properties to **P4P5P4-1**, and the isomeric tridomain compounds **P4M5P4-1** and **P4P5P4-1** independently aggregated and disaggregated at the amido and ethynyl domains. The homoaggregations of **M4P5M4-1** and **M4M5M4-1** should be identical to those of **P4M5P4-1** and **P4P5P4-1**, respectively, except for the inverted nature of the CD spectra.

**Heteroaggregation of P4M5P4-1/P4P5P4-1.** On the basis of the results of the homoaggregation of **P4M5P4-1** and **P4P5P4-1**, heteroaggregation was further studied. In such a study, it was critical to analyze the selectivities of heteroaggregation and homoaggregation.

It was first confirmed that the **P4M5P4-1/P4P5P4-1** mixture in THF was the random-coil state for both **P4M5P4-1** and **P4P5P4-1**. CD spectra (25 °C) of the 1:1 mixture of **P4M5P4-1** ( $2.5 \times 10^{-4}$  M) and **P4P5P4-1** ( $2.5 \times 10^{-4}$  M) coincided with the calculated spectrum obtained by adding the CD spectra of **P4M5P4-1** (Figure 6, THF) and **P4P5P4-1**<sup>9</sup> (THF) in the S-random-coil state (Figure S8a, Supporting Information). The UV-vis spectra also showed good agreement (Figure S8b). Then, trifluoromethylbenzene, which promotes the aggregation of both ethynyl and amido domain,<sup>10,11</sup> was added to make a solution of 10% THF/trifluoromethylbenzene (Figure 12).

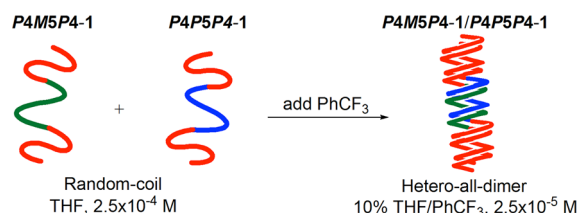


**Figure 12.** Formation of **P4M5P4-1/P4P5P4-1** heteroall-dimer.

The concentrations of **P4M5P4-1/P4P5P4-1** were adjusted to  $2.5 \times 10^{-6}$  or  $2.5 \times 10^{-5}$  M. The experimental CD and UV-vis spectra of the **P4M5P4-1/P4P5P4-1** mixture were quite different from those of the **P4M5P4-1/P4P5P4-1** mixture in the

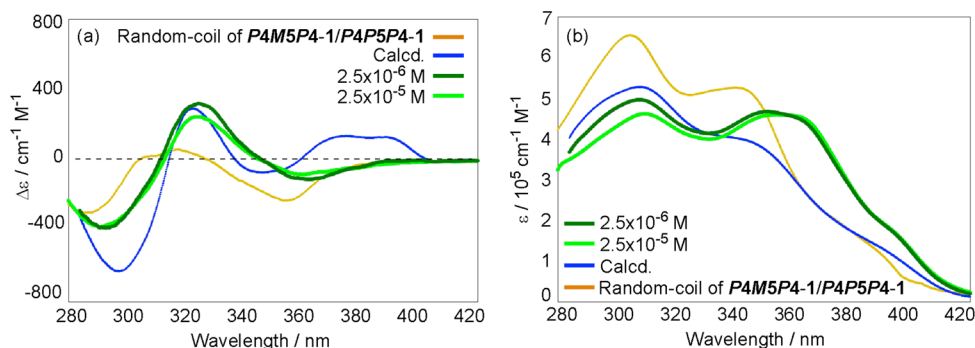


**Figure 13.** (a) CD and (b) UV-vis spectra of  $P4MSP4-1/P4PSP4-1$  in 10% THF/trifluoromethylbenzene (25 °C). The spectra of the random-coil state of  $P4MSP4-1/P4PSP4-1$  (Figure S8) are shown. Calculated spectra obtained by adding S-all-dimer of  $P4MSP4-1$  (Figure 6a, fluorobenzene) and  $P4PSP4-1$ <sup>9</sup> (fluorobenzene) are also shown.

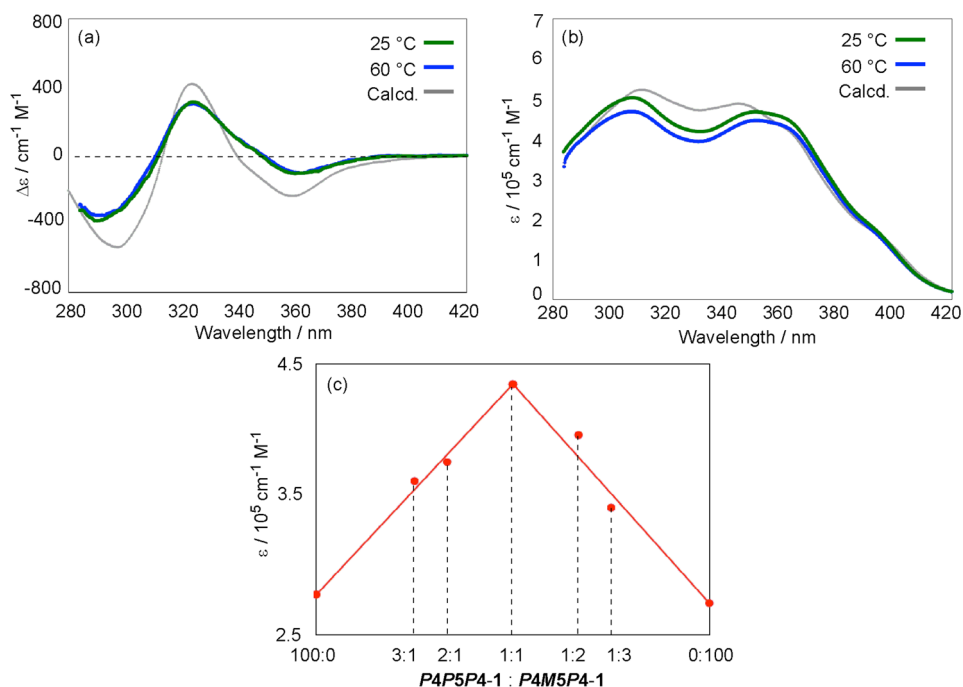


**Figure 14.** (a) CD and (b) UV-vis spectra of  $P4MSP4-1/P4PSP4-1$  in 10% THF/trifluoromethylbenzene ( $2.5 \times 10^{-6} \text{ M}$ , 25 °C). The calculated CD spectrum is that of aggregated (*P*)-4<sup>10</sup> (chloroform). The calculated UV-vis spectrum was obtained by adding the UV-vis spectrum of aggregated (*P*)-4 (Figure S9, chloroform) and heteroaggregated (*P*)-5/(*M*)-6<sup>13a</sup> (toluene) in 2:1 ratio. (c) Result of Job plot experiment (10% THF/trifluoromethylbenzene,  $2.5 \times 10^{-6} \text{ M}$ , 25 °C) using  $\epsilon$  (364 nm) against ratio of  $P4PSP4-1$  to  $P4MSP4-1$ .

random-coil state (Figure 13 and S8) and were also different from the calculated spectra obtained by adding those of S-all-dimers  $P4MSP4-1$  (Figure 6a, fluorobenzene) and  $P4PSP4-1$ <sup>9</sup> (fluorobenzene). The calculated CD spectrum of the heteroall-dimer, in which both the amido and ethynyl domains were aggregated, was obtained from that of aggregated (*P*)-4<sup>10</sup> (chloroform). Because the ethynyl domain of  $P4MSP4-1/P4PSP4-1$  is racemic, its structure was assumed not to reflect CD. Although the assumption is simple, the experimental CD spectrum was in fairly good agreement with the calculated spectrum (Figure 14a). The calculated UV-vis spectrum was obtained by adding the UV-vis spectrum of the aggregated (*P*)-4 (Figure S9, Supporting Information, chloroform) and that of heteroaggregated (*P*)-5/(*M*)-6<sup>13a</sup> (toluene) in 2:1 ratio. The experimental UV-vis spectra are in good agreement with the calculated spectrum (Figure 14b). Essentially the same results were obtained at a higher concentration of  $2.5 \times 10^{-5} \text{ M}$  (Figure 13). When the  $2.5 \times 10^{-6} \text{ M}$  solution was heated at 60 °C, no change was

observed in the CD or UV-vis spectrum, which indicated a high thermal stability of the heteroaggregate. The results indicated that  $P4MSP4-1/P4PSP4-1$  formed heteroall-dimer under the existing conditions. A Job plot experiment using UV absorption ( $2.5 \times 10^{-6} \text{ M}$ , 25 °C) at 364 nm in 10% THF/trifluoromethylbenzene revealed the formation of a 1:1 complex (Figure 14c).

HPLC analysis provided clear evidence of selective heteroaggregation without homoaggregation. An amido-dimer  $P4MSP4-1$  solution ( $2.5 \times 10^{-6} \text{ M}$ ) in 10% THF/trifluoromethylbenzene was prepared by adding trifluoromethylbenzene to the THF ( $2.5 \times 10^{-5} \text{ M}$ ) solution of  $P4MSP4-1$ . Normal-phase HPLC analysis using the same solvents revealed a retention time of 4.4 min for this mixture (Figure 15a). The same retention time was obtained for  $P4PSP4-1$  (Figure 15b). A  $P4MSP4-1/P4PSP4-1$  mixture in 10% THF/trifluoromethylbenzene, obtained as noted above showed a retention time of 3.5 min (Figure 15c). The coinjection of the  $P4MSP4-1/P4PSP4-1$

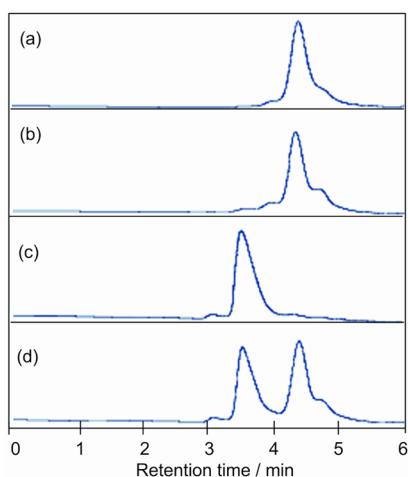


**Figure 15.** HPLC profiles of (a) *P4MSP4-1*, (b) *P4PSP4-1*, (c) *P4MSP4-1/P4PSP4-1* obtained as noted in text, and (d) coinjection mixture of a and c in 10% THF/trifluoromethylbenzene at room temperature. Mobile phase: 10% THF/trifluoromethylbenzene; flow rate: 0.5 mL/min; UV: 290 nm; column:  $3.9 \times 300$  mm  $\mu$ porasil; sample concentration:  $2.5 \times 10^{-6}$  M.

mixture and *P4MSP4-1* showed two peaks at 3.5 and 4.4 min, confirming the formation of different species in the *P4MSP4-1/P4PSP4-1* mixture and *P4MSP4-1* or *P4PSP4-1* (Figure 15d). The results indicated the heteroaggregate formation of *P4MSP4-1/P4PSP4-1* and essentially no homoaggregate formation. DLS analysis of this state of *P4MSP4-1/P4PSP4-1* (10% THF/trifluoromethylbenzene,  $5 \times 10^{-5}$  M, 20 °C) was conducted (Figure 16), and the heteroall-dimer state showed a 25 nm

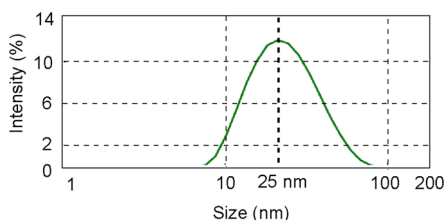


**Figure 16.** Size distributions of *P4MSP4-1/P4PSP4-1* determined by DLS experiments in 10% THF/trifluoromethylbenzene ( $5 \times 10^{-5}$  M, 20 °C).

average diameter, which was similar to that of the homoall-dimer state of *P4MSP4-1* (Figure 7). AFM analysis of the heteroall-dimer state was also conducted (Figure S10, Supporting Information). AFM images of the sample prepared from the *P4MSP4-1/P4PSP4-1* mixture (10% THF/trifluoromethylbenzene) showed dispersed particles of about 25 nm diameter. The results were in good agreement with DLS analysis. The homoaggregation of *P4PSP4-1*,<sup>9</sup> *P4MSP4-1* and the heteroaggregation of *P4MSP4-1/P4PSP4-1* were shown to possess a similar size, which was consistent with dimeric heteroaggregate formation and not higher aggregates.

The solvent effect on aggregation was examined by CD spectroscopy using the same procedures starting from the THF solution of the S-random-coil states of *P4MSP4-1/P4PSP4-1*. When fluorobenzene or chloroform was added to form 10% THF solution, CD and UV-vis spectra similar to those in the experiment using trifluoromethylbenzene were obtained. The results indicated the formation of the heteroall-dimer (Figure S11, Supporting Information). The addition of toluene or bromobenzene gave similar CD spectra but different UV-vis

spectra with reduced absorbance at 360 nm (Figure S12, Supporting Information), which may be due to disaggregation at the ethynyl domain to form the heteroamido-dimer state.

It was then considered interesting to determine whether the initial states of *P4MSP4-1* and *P4PSP4-1* affect the heteroaggregate formation. The above procedures initiated the aggregation from the S-random-coil states of *P4MSP4-1* and *P4PSP4-1* in THF with the addition of trifluoromethylbenzene. Then, the aggregation experiment was started from the S-amido-dimer states of *P4MSP4-1* (Figure 3) and *P4PSP4-1*<sup>9</sup> in 10% THF/trifluoromethylbenzene. Two solutions ( $2.5 \times 10^{-6}$  M) of *P4MSP4-1* and *P4PSP4-1* in 10% THF/trifluoromethylbenzene were prepared and mixed at room temperature. The experimental CD and UV-vis spectra of the mixture were different from those of the heteroall-dimer of *P4MSP4-1/P4PSP4-1* (Figure S13, Supporting Information) but identical to the calculated spectra obtained by adding those of the S-amido-dimer states of *P4MSP4-1* (Figure 6a, bromobenzene) and *P4PSP4-1*<sup>9</sup> (bromobenzene). HPLC analysis of this mixture gave a retention time of 4.4 min, different from the retention time (3.5 min) of *P4MSP4-1/P4PSP4-1* heteroaggregation (Figure S14, Supporting Information). The results showed no heteroaggregation; heteroaggregation occurred only in the random-coil, not in the amido-dimer (Figure 17).

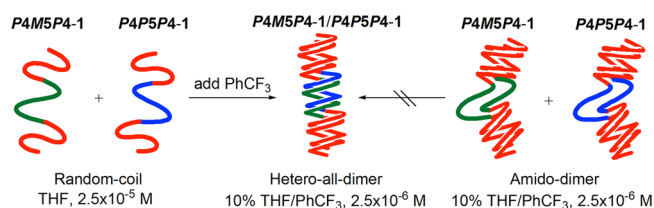


**Figure 17.** *P4MSP4-1/P4PSP4-1* heteroall-dimer formation from random-coil.

As for the mechanism of heteroall-dimer formation, it may be likely that heteroaggregation initially occurred at the central ethynyl domain with the addition of trifluoromethylbenzene, which was followed by the aggregation at the terminal amido domain. In the case that the aggregation at the amido domain preceded that at the ethynyl domain, a mixture of heteroaggregates and homoaggregates formed (Figure 18).

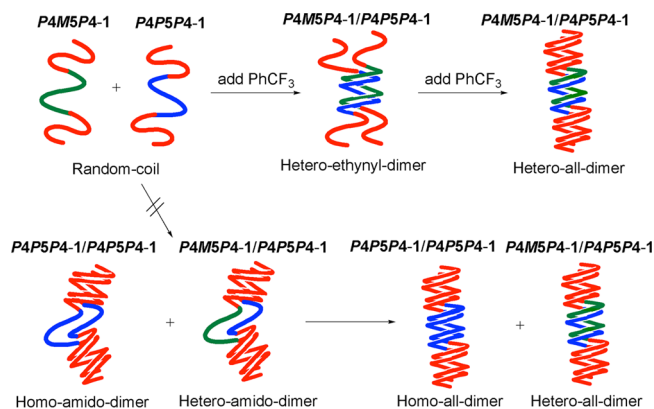


**Figure 18.** Mechanism of *P4MSP4-1/P4PSP4-1* heteroall-dimer formation.

The process of addition of trifluoromethylbenzene to the THF solution of *P4MSP4-1/P4PSP4-1* was followed by CD

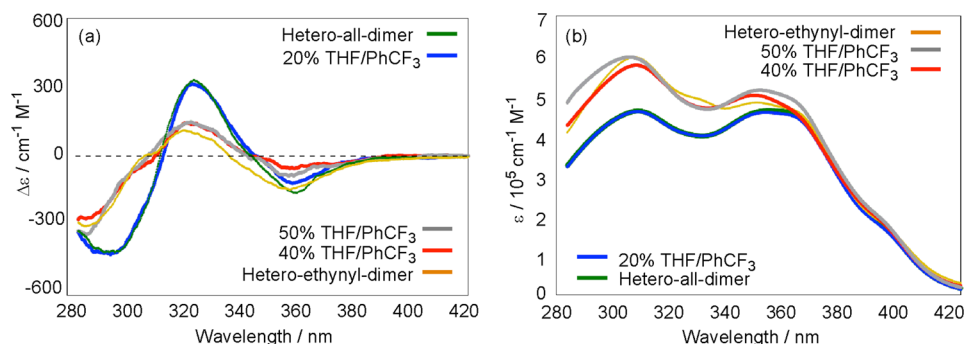


**Figure 19.** (a) CD and (b) UV–vis spectra of *P4M5P4-1/P4P5P4-1* in 20% THF/trifluoromethylbenzene, 40% THF/trifluoromethylbenzene, and 50% THF/trifluoromethylbenzene ( $2.5 \times 10^{-6}$  M, 25 °C). The spectra of the heteroall-dimer (Figure 14) and heteroethynyl-dimer (Figure 21) of *P4M5P4-1/P4P5P4-1* are also shown.

(Figure 19). The 50% and 40% THF/trifluoromethylbenzene solutions ( $2.5 \times 10^{-6}$  M) were prepared by adding trifluoromethylbenzene to the THF solution, which exhibited CD and UV–vis spectra of heteroethynyl-dimer, vide infra (Figure 21). The CD spectra with 20% THF content coincided with those of the heteroall-dimer (Figure 14), and the results indicated the two-step mechanism of the heteroall-dimer formation of *P4M5P4-1/P4P5P4-1* (Figure 18). It was shown that *P4M5P4-1* and *P4P5P4-1* selectively formed the heteroall-dimer state, when their THF solution was diluted with trifluoromethylbenzene at room temperature.

Along with the heteroall-dimer, a heteroethynyl-dimer was formed for *P4M5P4-1/P4P5P4-1* with a change in the procedures. Solutions of *P4M5P4-1* and *P4P5P4-1*<sup>9</sup> ( $2.5 \times 10^{-5}$  M) in 12% DMSO/trifluoromethylbenzene, both in ethynyl-dimer states (Figure 6), were mixed in 1:1 ratio at room temperature. The solution was heated at 80 °C for 10 min to form random-coils and cooled to 25 °C to form heteroethynyl-dimers (Figure 20).

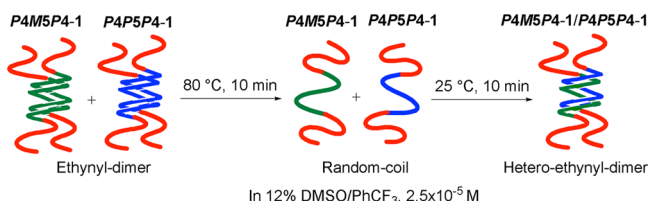


**Figure 20.** Formation of *P4M5P4-1/P4P5P4-1* heteroethynyl-dimer from ethynyl-dimer.

The CD and UV–vis spectra of the resulted solution were apparently different from those of the *P4M5P4-1/P4P5P4-1* heteroall-dimer (Figure 21). The CD spectrum of the *P4M5P4-1/P4P5P4-1* heteroethynyl-dimer was calculated using that of disaggregated (*P*)-4<sup>9</sup> (THF), which was in fair agreement with the experimental spectra (Figure 21a). UV–vis spectrum was calculated by adding the UV–vis spectrum of disaggregated (*P*)-4 (Figure S9, THF) and that of heteroaggregated (*P*)-5/(*M*)-6<sup>13a</sup> (toluene) in 2:1 ratio, which was again in agreement with the experimental spectrum (Figure 21b). The Job plot experiment using UV–vis absorption at 364 nm showed the formation of a 1:1 complex (Figure 21c). This state was concluded as the heteroethynyl-dimer state of *P4M5P4-1/P4P5P4-1*.

HPLC analysis of the heteroethynyl-dimer state was conducted. A solution ( $5 \times 10^{-5}$  M) of *P4M5P4-1/P4P5P4-1* in 12% DMSO/trifluoromethylbenzene was prepared by mixing

*P4P5P4-1* and *P4M5P4-1* at room temperature. A retention time of the resulting solution of 4.1 min was obtained (Figure 22a). When the solution was heated at 80 °C and cooled to room temperature, HPLC analysis showed a retention time of 3.3 min (Figure 22b). The heteroethynyl-dimer state of *P4M5P4-1/P4P5P4-1* was thus confirmed.

*P4M5P4-1/P4P5P4-1* was in the random-coil state in THF-*d*<sub>8</sub> (Figure S8), and the <sup>1</sup>H NMR spectrum ( $2 \times 10^{-4}$  M, 25 °C) showed two sharp amide protons at  $\delta$  10.0 and 10.2 as well as well-resolved aromatic protons (Figure S15a, Supporting Information). The spectrum of the heteroethynyl-dimer in 12% DMSO-*d*<sub>6</sub>/PhCF<sub>3</sub>-*d*<sub>5</sub> (Figure 21) showed relatively sharp amide peaks at  $\delta$  11.2 and 11.4 (Figure S15b). *P4M5P4-1/P4P5P4-1* in 10% THF-*d*<sub>8</sub>/CDCl<sub>3</sub> is in the heteroall-dimer state (Figure S11) and showed a serious broadening of both amide and aromatic protons (Figure S15c). Similar results were obtained in the homoaggregates of *P4P5P4-1*<sup>9</sup>.

A study of the structural change of heteroaggregates between the heteroall-dimer and the heteroethynyl-dimer was conducted. To a 10% THF/trifluoromethylbenzene solution ( $2.5 \times 10^{-6}$  M) of *P4M5P4-1/P4P5P4-1* in the heteroall-dimer state was added DMSO. When DMSO content was increased from 0% to 30%, the CD intensity in the 290 and 320 nm region decreased (Figure S16a,b, Supporting Information). The UV–vis intensity in the 300 nm region increased. The spectra did not change at DMSO contents above 20%, and they are in good agreement with those of the heteroethynyl-dimer (Figure S16c,d). The result showed disaggregation at the amido domain with the DMSO addition (Figure 23).

*P4M5P4-1/P4P5P4-1* formed dimeric heteroaggregates but not homoaggregates. The heteroaggregates were thermally more stable than homoaggregates of *P4M5P4-1* and *P4P5P4-1*. To form heteroaggregates *P4M5P4-1/P4P5P4-1*, homoaggregates *P4M5P4-1* and *P4P5P4-1* need to disaggregate to random-coil, and then the heteroaggregation occurs by a two-step mechanism via initial aggregation at the central ethynyl domain. Thus, the strong and initial heteroaggregation at the ethynyl domain may be the origin of the predominant heteroaggregation over homoaggregation.

**Racemic Heteroaggregation of *P4P5P4-1/M4M5M4-1* and *P4M5P4-1/M4P5M4-1*.** The heteroaggregation of *P4P5P4-1/M4M5M4-1*, which is a racemic mixture, was also examined (Figure 24). To a THF solution ( $2.5 \times 10^{-5}$  M) of *P4P5P4-1* and *M4M5M4-1*, trifluoromethylbenzene was added, and 10% THF/trifluoromethylbenzene solution ( $2.5 \times 10^{-6}$  M) was prepared. The solution was not CD-active. UV–vis spectrum showed an increase in absorbance in the 360 nm region, which



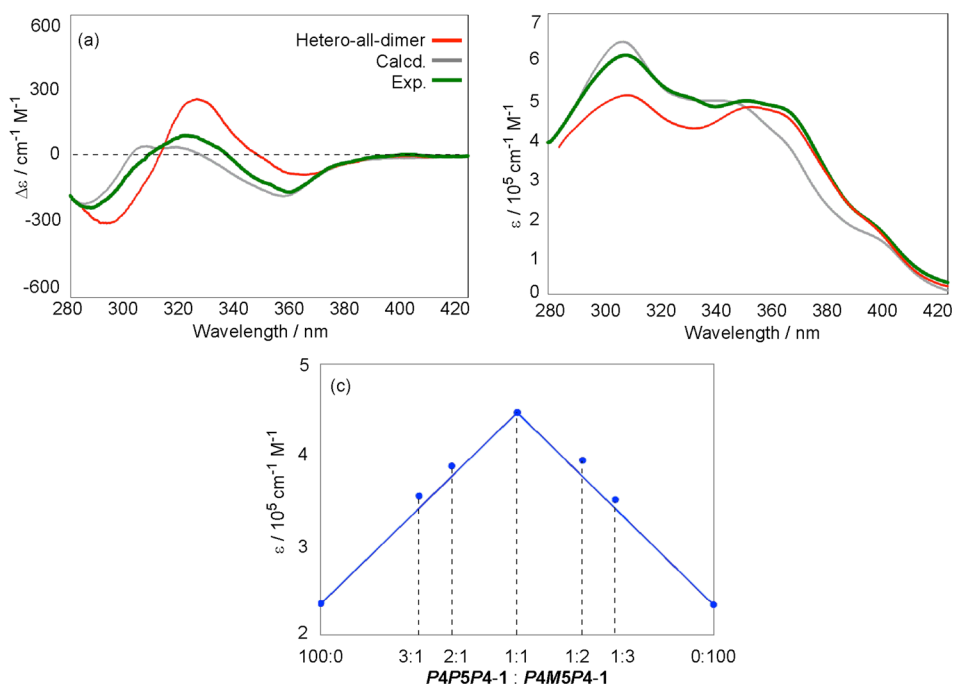


**Figure 21.** (a) CD and (b) UV–vis spectra of *P4M5P4-1/P4P5P4-1* in 12% DMSO/trifluoromethylbenzene ( $2.5 \times 10^{-5}$  M, 25 °C). The calculated CD spectrum was obtained from the CD spectrum of disaggregated (*P*)-4<sup>9</sup> (THF). The calculated UV–vis spectrum was obtained by adding the UV–vis spectrum of disaggregated (*P*)-4 (Figure S9, THF) and heteroaggregated (*P*)-5/(*M*)-6<sup>13a</sup> (toluene) in 2:1 ratio. The spectra of *P4M5P4-1/P4P5P4-1* heteroall-dimer (Figure 14) are also shown. (c) Result of Job plot experiment (12% DMSO/trifluoromethylbenzene,  $2.5 \times 10^{-5}$  M, 25 °C) using  $\epsilon$  (364 nm) against ratio of *P4P5P4-1* to *P4M5P4-1*.

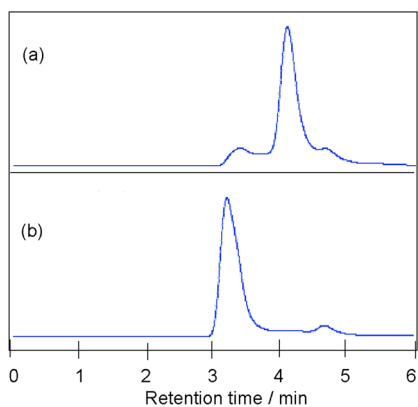


**Figure 22.** HPLC profiles of *P4M5P4-1/P4P5P4-1* in 12% DMSO/trifluoromethylbenzene at room temperature (a) before heating and (b) after heating at 80 °C for 10 min. Mobile phase: 12% DMSO/trifluoromethylbenzene; flow rate: 0.5 mL/min; UV: 290 nm; column:  $3.9 \times 300$  mm  $\mu$ porasil; sample concentration:  $5 \times 10^{-5}$  M.

was quite different from that observed in the random-coil (Figure 25a). The Job plot experiment using UV absorption ( $2.5 \times 10^{-6}$  M, 25 °C) at 364 nm in 10% THF/trifluoromethylbenzene revealed the formation of a 1:1 complex (Figure 25b). These results suggested heteroaggregate formation at the ethynyl domain. Similar observations were made using fluorobenzene. HPLC analysis of 10% THF/trifluoromethylbenzene solution indicated heteroaggregate formation with a retention time of 3.5 min, with no homoaggregate formation (Figure 26). DLS and AFM analyses provided about 25 nm average diameter, which was consistent with heteroall-dimer formation (Figure 27, and Figure S17, Supporting Information).

To determine the aggregate state at the amido domain, DMSO addition was carried out. To a 10% THF/trifluoromethylbenzene

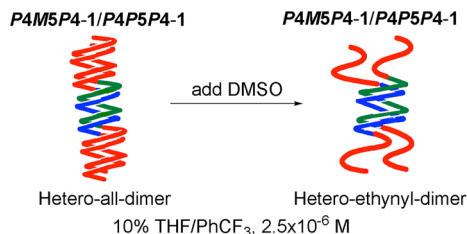


**Figure 23.** Structure change of *P4M5P4-1/P4P5P4-1* heteroall-dimer to heteroethynyl-dimer.

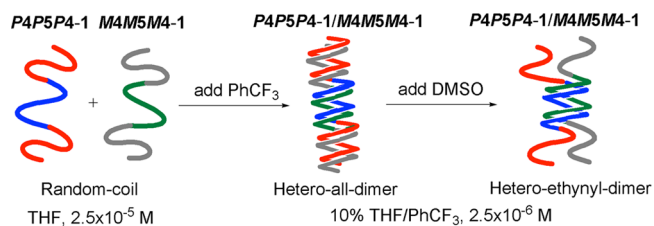


**Figure 24.** Racemic heteroaggregation of *P4P5P4-1/M4M5M4-1*.

solution ( $2.5 \times 10^{-6}$  M) of *P4P5P4-1/M4M5M4-1*, DMSO was added. An increase in DMSO content from 0 to 20% increased UV–vis intensity in the 300 nm region with an isosbestic point at 343 nm (Figure 28). These experimental results were consistent with disaggregation at the amido domain of the heteroall-dimer of *P4P5P4-1/P4M5P4-1* (Figure S16b), consistent with the heteroall-dimer formation of *P4P5P4-1/M4M5M4-1* in 10% THF/trifluoromethylbenzene. Analysis of *P4M5P4-1/M4P5M4-1* provided the same results of heteroaggregation (Figures S18–22, Supporting Information).

Note that *P4P5P4-1/P4M5P4-1*, *P4P5P4-1/M4M5M4-1*, and *P4M5P4-1/M4P5M4-1* formed heteroaggregates but did

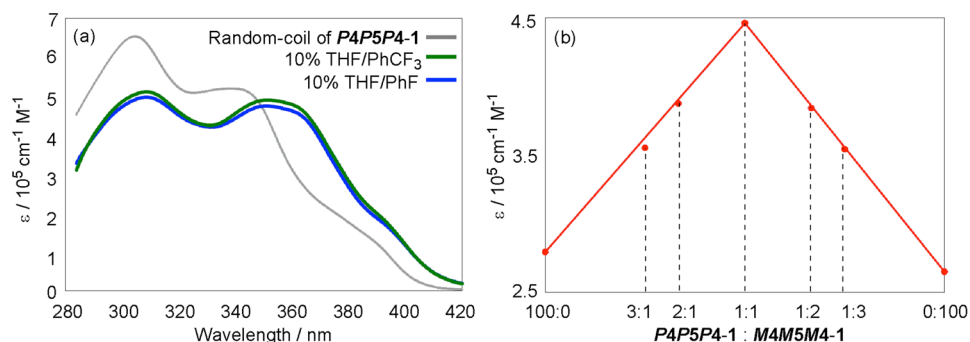


**Figure 25.** (a) UV–vis spectra of *P4P5P4-1*/*M4M5M4-1* in 10% THF/trifluoromethylbenzene and 10% THF/fluorobenzene ( $2.5 \times 10^{-6}$  M, 25 °C). The UV spectrum of the random-coil of *P4P5P4-1*<sup>9</sup> (THF) is also shown. (b) Job plot experiment (10% THF/trifluoromethylbenzene,  $2.5 \times 10^{-6}$  M, 25 °C) using  $\epsilon$  (364 nm) against ratio of *P4P5P4-1* to *M4M5M4-1*.

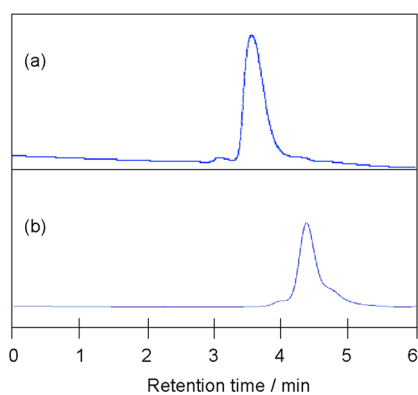


**Figure 26.** HPLC profiles of (a) *P4P5P4-1*/*M4M5M4-1* and (b) *P4P5P4-1* in 10% THF/trifluoromethylbenzene at room temperature. Mobile phase: 10% THF/trifluoromethylbenzene; flow rate: 0.5 mL/min; UV: 290 nm; column:  $3.9 \times 300$  mm  $\mu$ porasil; sample concentration:  $2.5 \times 10^{-6}$  M.

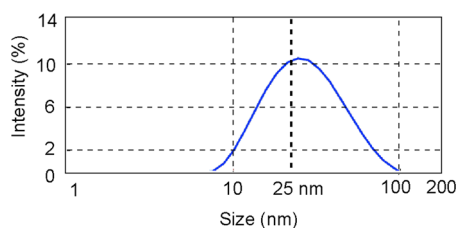


**Figure 27.** Size distributions of *P4P5P4-1*/*M4M5M4-1* determined by DLS experiments in 10% THF/trifluoromethylbenzene ( $5 \times 10^{-5}$  M, 20 °C).

not form homoaggregates. In the case of oligomers with central ethynyl domains containing enantiomer pairs, heteroaggregation predominates homoaggregation. A comparison of the three combinations revealed a relatively small effect of the aggregation of the amido domain on the aggregation of the tridomain compounds.

**Aggregation of *P4P5P4-1*/*M4P5M4-1*.** The aggregation of *P4P5P4-1*/*M4P5M4-1* was examined, in which *P4P5P4-1* and *M4P5M4-1* had the central part of the (*P*)-ethynyl domain and a racemic nature of the amido domain. To a solution ( $2.5 \times 10^{-5}$  M) of *P4P5P4-1* and *M4P5M4-1* in THF was added trifluoromethylbenzene, and 10% THF/trifluoromethylbenzene solution ( $2.5 \times 10^{-6}$  M) was prepared. The CD spectrum (25 °C) of *P4P5P4-1*/*M4P5M4-1* showed a weak Cotton effect similar to that of disaggregated (*P*)-**5**<sup>11a</sup> (chloroform) (Figure S23a, Supporting Information). The

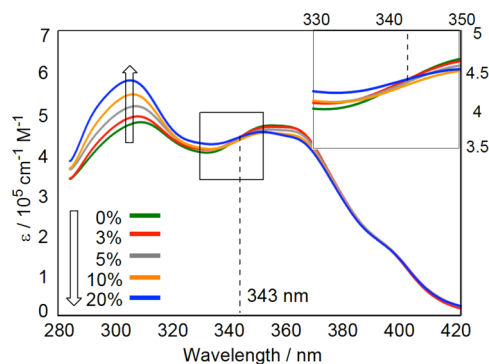


**Figure 28.** UV spectra ( $2.5 \times 10^{-6}$  M, 25 °C) of *P4P5P4-1*/*M4M5M4-1* in 10% THF/trifluoromethylbenzene, to which DMSO was added. DMSO content was changed between 0 and 20%. The inset shows the expansion of the spectrum between 330 and 350 nm.

UV–vis ( $2.5 \times 10^{-6}$  M, 25 °C) spectrum was different from that of the S-random coil state of *P4P5P4-1*. The retention time of 4.4 min was obtained in the HPLC analysis using the same solvent (Figure S24, Supporting Information). Although *P4P5P4-1*/*M4P5M4-1* was confirmed to form aggregates, homoaggregation and heteroaggregation of *P4P5P4-1*/*M4P5M4-1* could not be distinguished.

## CONCLUSION

To summarize, four possible combinations of tridomain compounds, i.e., *P4P5P4-1*/*P4M5P4-1*, *P4P5P4-1*/*M4M5M4-1*, *P4M5P4-1*/*M4P5M4-1*, and *P4P5P4-1*/*M4P5M4-1*, were examined for heteroaggregation. Three of them, i.e., *P4P5P4-1*/*P4M5P4-1*, *P4P5P4-1*/*M4M5M4-1*, and *P4M5P4-1*/*M4P5M4-1*, formed dimeric heteroaggregates but not homoaggregates. This is a notable example of synthetic multidomain compounds that are selective for forming heteroaggregates. The heteroaggregation of the central ethynyl domain with an enantiomeric structure appears to govern the heteroaggregation of each tridomain compound. This may be due to the stronger heteroaggregation compared with homoaggregation at this domain, and to the procedures containing the initial aggregation at the ethynyl domain. It will be interesting to examine whether proteins employ related strategies for heteroaggregation.

## EXPERIMENTAL SECTION

**General Methods.** <sup>1</sup>H NMR spectra were recorded on a 400 MHz spectrometer with tetramethylsilane as an internal standard. <sup>13</sup>C NMR spectra were recorded on a 151 MHz spectrometer. <sup>1</sup>H NMR spectra

taken in THF- $d_8$  ( $\delta$  1.73) and  $^{13}\text{C}$  NMR spectra taken in THF- $d_8$  ( $\delta$  67.4) were referenced to the residual solvents. MALDI TOF-MS spectra were obtained with negative ion mode and using 2-amino-5-nitropyridine as a matrix. CD and UV-vis spectra were recorded using distilled or spectrophotometric grade commercial solvents.

**Typical Procedures for the Synthesis of Amido-ethynyl-amidohelicene Tridomain Oligomer.** Under an argon atmosphere, a mixture of  $2^9$  (50 mg, 0.017 mmol), tris(dibenzylideneacetone)-dipalladium(0) chloroform adduct (4.6 mg, 0.0086 mmol), cuprous iodide (9.6 mg, 0.10 mmol), trimesitylphosphine (10 mg, 0.052 mmol), triphenylphosphine (6.8 mg, 0.052 mmol), tetrabutylammonium iodide (32 mg, 0.086 mmol), triethylamine (0.1 mL), and *N,N*-dimethylformamide (1 mL) was freeze-evacuated three times. A solution of  $3^{11}$  (22 mg, 0.0086 mmol) in THF (1 mL) was also freeze-evacuated three times and then added dropwise to the above solution. The mixture was stirred for 5 h at 45 °C. The reaction was quenched by adding saturated aqueous ammonium chloride, and the organic materials were extracted with ethyl acetate and toluene. The organic layer was washed with water and brine and dried over magnesium sulfate. The solvents were evaporated under reduced pressure. Separation by recycling GPC and silica gel chromatography followed by precipitation from hexane-dichloromethane gave **1** as a yellow solid.

**Tridomain Oligomer P4M5P4-1.** Yield 45 mg, 0.0056 mmol, 65%. Mp 246–251 °C (hexane–dichloromethane).  $[\alpha]_D^{23}$  –94 (c 0.05, PhBr). MS (MALDI-TOF, 2-amino-5-nitropyridine) Calcd for  $^{12}\text{C}_{539}^{13}\text{C}_5\text{H}_{553}\text{N}_{18}\text{O}_{48}$   $[\text{M} - \text{H}]^-$ : 8110.2. Found: 8110.8. UV-vis (THF,  $2.5 \times 10^{-6}$  M)  $\lambda_{\text{max}}$  ( $\epsilon$ ) 340 nm ( $5.1 \times 10^5$ ). CD (THF,  $2.5 \times 10^{-6}$  M)  $\lambda$  ( $\Delta\epsilon$ ) 315 nm (148), 350 nm (–244), 389 nm (220). IR (KBr) 2924, 2852, 2208, 1722, 1653  $\text{cm}^{-1}$ . Anal. ( $\text{C}_{544}\text{H}_{554}\text{N}_{18}\text{O}_{48}$ ) Calcd for: C, 80.54; H, 6.88; N, 3.11%. Found: C, 80.40; H, 7.04; N, 3.33%.  $^1\text{H}$  NMR (400 MHz, THF- $d_8$ )  $\delta$  0.84 (42H, m), 1.27–1.51 (214H, m), 1.76–1.89 (28H, m), 1.96 (78H, s), 4.26–4.43 (28H, m), 7.48–7.55 (27H, m), 7.63–7.70 (17H, m), 7.72–7.78 (10H, m), 7.97 (2H, s), 8.11 (4H, s), 8.22–8.29 (9H, m), 8.32–8.45 (42H, m), 8.58–8.62 (9H, m), 8.78–8.85 (9H, m) 10.02 (2H, s), 10.20 (16H, s).  $^{13}\text{C}$  NMR (151 MHz, THF- $d_8$ )  $\delta$  14.4, 23.45, 23.52, 23.55, 27.0, 28.6, 29.71, 29.74, 29.8, 30.26, 30.31, 30.5, 32.83, 32.85, 65.5, 65.7, 66.0, 66.3, 80.0, 89.1, 90.2, 93.7, 93.8, 94.8, 114.0, 115.2, 115.6, 116.7, 120.8, 120.87, 120.89, 121.2, 121.5, 124.1, 124.6, 125.1, 125.3, 125.4, 125.5, 127.1, 127.5, 127.7, 127.9, 127.95, 128.05, 128.26, 128.32, 128.4, 128.5, 129.8, 129.88, 129.93, 130.20, 130.24, 130.3, 130.7, 130.9, 131.0, 131.07, 131.14, 131.9, 132.1, 132.25, 132.30, 132.5, 132.7, 132.8, 132.9, 133.0, 133.19, 133.24, 133.3, 135.8, 136.2, 136.3, 137.49, 137.55, 137.6, 137.77, 137.80, 139.01, 139.05, 141.2, 141.4, 141.6, 153.6, 165.4, 165.8, 166.5, 167.9, 168.1, 168.2.

**Tridomain Oligomer M4P5M4-1.** Yield 43 mg, 0.0053 mmol, 61%. Mp 245–247 °C (hexane–dichloromethane).  $[\alpha]_D^{23}$  +74 (c 0.05, PhBr). Anal. ( $\text{C}_{544}\text{H}_{554}\text{N}_{18}\text{O}_{48}$ ) Calcd for: C, 80.54; H, 6.88; N, 3.11%. Found: C, 80.17; H, 7.02; N, 3.11%.

**Tridomain Oligomer M4M5M4-1.** Yield 40 mg, 0.0049 mmol, 54%. Mp 246–248 °C (hexane–dichloromethane).  $[\alpha]_D^{23}$  +327 (c 0.25, THF). Anal. ( $\text{C}_{544}\text{H}_{554}\text{N}_{18}\text{O}_{48}$ ) Calcd for: C, 80.54; H, 6.88; N, 3.11%. Found: C, 80.16; H, 7.21; N, 3.10%.

**Procedures for CD and UV-vis Analyses of P4M5P4-1.** (Figures 3, 4, 5, 6, 9, 11, S1, S2, S3, S4, S5, S6, and S7). Solutions of P4M5P4-1 were prepared at room temperature, sonicated, and put in a quartz cell for measurement. For variable temperature experiment, the solution was heated at the highest temperature noted in each Figure, and was gradually cooled to lower temperatures.

**Procedures for DLS Measurements of P4M5P4-1.** (Figure 7). Solutions of P4M5P4-1 ( $5 \times 10^{-5}$  M) in THF, bromobenzene, 12% DMSO/trifluoromethylbenzene, and fluorobenzene were prepared. DLS measurements were carried out at 20 °C. Solvents were used after filtration through 0.2  $\mu\text{m}$  pore membrane filters.

**Procedures for CD and UV-vis Analyses of P4M5P4-1/P4P5P4-1.** Solutions of P4M5P4-1 ( $2.5 \times 10^{-4}$  M) and P4P5P4-1 ( $2.5 \times 10^{-4}$  M) in THF were prepared. The solutions were mixed in 1:1 v/v at room temperature, and the analyses were carried out at 25 °C (Figure S8).

Solutions of P4M5P4-1 ( $2.5 \times 10^{-4}$  M or  $2.5 \times 10^{-5}$  M) and P4P5P4-1 ( $2.5 \times 10^{-4}$  M or  $2.5 \times 10^{-5}$  M) in THF were prepared. The solutions of P4M5P4-1 (0.5 mL) and P4P5P4-1 (0.5 mL) were mixed in a volumetric flask (10 mL) at room temperature, to which trifluoromethylbenzene was added to make a 10 mL solution. The solution was noted 10% THF/trifluoromethylbenzene with concentrations of  $2.5 \times 10^{-5}$  M and  $2.5 \times 10^{-6}$  M in this work. The analyses were carried out at 25 °C and 60 °C (Figure 13 and 14).

Solutions of P4M5P4-1 ( $2.5 \times 10^{-5}$  M) and P4P5P4-1 ( $2.5 \times 10^{-5}$  M) in THF were prepared. The solutions of P4M5P4-1 (0.5 mL) and P4P5P4-1 (0.5 mL) were mixed in a volumetric flask (10 mL) at room temperature, to which a solvent (fluorobenzene, chloroform, toluene, or bromobenzene) was added to make a solution (10 mL) of 10% THF with concentration of  $2.5 \times 10^{-6}$  M. Analyses were carried out at 25 °C (Figures S11 and S12).

Solutions of P4M5P4-1 ( $2.5 \times 10^{-6}$  M) and P4P5P4-1 ( $2.5 \times 10^{-6}$  M) in 10% THF/trifluoromethylbenzene were prepared. The solutions of P4M5P4-1 and P4P5P4-1 were mixed in 1:1 v/v at room temperature, and analyses were carried out at 25 °C (Figure S13).

Solutions of P4M5P4-1 ( $1.25 \times 10^{-5}$  M) and P4P5P4-1 ( $1.25 \times 10^{-5}$  M) in THF were prepared. The solutions of P4M5P4-1 (1 mL) and P4P5P4-1 (1 mL) were mixed in volumetric flasks (10 mL) at room temperature, to which trifluoromethylbenzene and THF were added to make solutions (10 mL) of 20% THF/trifluoromethylbenzene, 40% THF/trifluoromethylbenzene, and 50% THF/trifluoromethylbenzene with concentration of  $2.5 \times 10^{-6}$  M. Analyses were carried out at 25 °C (Figure 19).

Solutions of P4M5P4-1 ( $2.5 \times 10^{-5}$  M) and P4P5P4-1 ( $2.5 \times 10^{-5}$  M) in 12% DMSO/trifluoromethylbenzene were prepared. The solutions of P4M5P4-1 and P4P5P4-1 were mixed in 1:1 v/v at room temperature, and the mixture was heated at 80 °C for 10 min. Analyses were carried out after cooling to 25 °C (Figure 21).

Solutions of P4M5P4-1 ( $2.5 \times 10^{-5}$  M) and P4P5P4-1 ( $2.5 \times 10^{-5}$  M) in THF were prepared. The solutions of P4M5P4-1 (0.5 mL) and P4P5P4-1 (0.5 mL) were mixed in a volumetric flask (10 mL) at room temperature, to which trifluoromethylbenzene was added to make a solution (10 mL) of 10% THF/trifluoromethylbenzene with concentration of  $2.5 \times 10^{-6}$  M. This solution (2 mL) was put in a quartz cell, and DMSO (0.02, 0.06, 0.1, 0.2, 0.4, and 0.6 mL) was added using microsyringe. These solutions were noted, in this work, 1%, 3%, 5%, 10%, 20%, and 30% DMSO content in 10% THF/trifluoromethylbenzene solutions, respectively. Analyses were carried out at 25 °C (Figure S16).

**Procedures for HPLC Measurements of P4M5P4-1/P4P5P4-1.** Solutions of P4M5P4-1 ( $2.5 \times 10^{-6}$  M) and P4P5P4-1 ( $2.5 \times 10^{-6}$  M) in 10% THF/trifluoromethylbenzene were prepared, and the measurements were carried out at room temperature (Figure 15a,b).

Solutions of P4M5P4-1 ( $2.5 \times 10^{-5}$  M) and P4P5P4-1 ( $2.5 \times 10^{-5}$  M) in THF were prepared. The solutions of P4M5P4-1 (0.5 mL) and P4P5P4-1 (0.5 mL) were mixed in a volumetric flask (10 mL) at room temperature, to which trifluoromethylbenzene was added to make a solution (10 mL) of 10% THF/trifluoromethylbenzene with concentration of  $2.5 \times 10^{-6}$  M. The measurement was carried out at room temperature (Figures 15c and S14b).

Solutions of P4M5P4-1 ( $2.5 \times 10^{-6}$  M) and P4P5P4-1 ( $2.5 \times 10^{-6}$  M) in 10% THF/trifluoromethylbenzene were prepared. The solutions of P4M5P4-1 and P4P5P4-1 were mixed in 1:1 v/v, and the measurement was carried out at room temperature (Figures 15d and S14a).

Solutions of P4M5P4-1 ( $5 \times 10^{-5}$  M) and P4P5P4-1 ( $5 \times 10^{-5}$  M) in 12% DMSO/trifluoromethylbenzene were prepared. The solutions of P4M5P4-1 and P4P5P4-1 were mixed in 1:1 v/v, and the measurement was carried out at room temperature (Figure 22a). This mixture was heated at 80 °C for 10 min, and the measurement was carried out after cooling to room temperature (Figure 22b).

**Procedures for DLS Measurements of P4M5P4-1/P4P5P4-1.** Solutions of P4M5P4-1 ( $5 \times 10^{-4}$  M) and P4P5P4-1 ( $5 \times 10^{-4}$  M) in THF were prepared. The solutions of P4M5P4-1 (0.1 mL) and P4P5P4-1 (0.1 mL) were mixed in a grass vial at room temperature, to which trifluoromethylbenzene was added to make a solution (10 mL)



of 10% THF/trifluoromethylbenzene with concentration of  $5 \times 10^{-5}$  M. The DLS measurements were carried out at 20 °C (Figure 16). Solvents were used after filtration through 0.2  $\mu\text{m}$  pore membrane filters.

**Procedures for  $^1\text{H}$  NMR Analysis of  $\text{P4M5P4-1/P4P5P4-1}$ .** Solutions of  $\text{P4M5P4-1}$  ( $2 \times 10^{-4}$  M) and  $\text{P4P5P4-1}$  ( $2 \times 10^{-4}$  M) in THF- $d_8$  were prepared. The solutions of  $\text{P4M5P4-1}$  and  $\text{P4P5P4-1}$  were mixed in 1:1 v/v. The measurement was carried out after cooling to 25 °C (Figure S15a).

Solutions of  $\text{P4M5P4-1}$  ( $2 \times 10^{-4}$  M) and  $\text{P4P5P4-1}$  ( $2 \times 10^{-4}$  M) in 12% DMSO- $d_6$ /PhCF $_3$ - $d_5$  were prepared. The solutions of  $\text{P4M5P4-1}$  and  $\text{P4P5P4-1}$  were mixed in 1:1 v/v, this mixture was heated at 80 °C for 10 min, and the measurement was carried out after cooling to 25 °C (Figure S15b).

Solutions of  $\text{P4M5P4-1}$  ( $2 \times 10^{-3}$  M) and  $\text{P4P5P4-1}$  ( $2 \times 10^{-3}$  M) in THF- $d_8$  were prepared. The solutions of  $\text{P4M5P4-1}$  (0.05 mL) and  $\text{P4P5P4-1}$  (0.05 mL) were mixed in a grass vial at room temperature, to which CDCl $_3$  was added to make a solution (1 mL) of 10% THF- $d_8$ /CDCl $_3$  with concentration of  $2 \times 10^{-4}$  M. The measurements were carried out at 25 °C (Figure S15c).

**Procedures for AFM Analysis of  $\text{P4M5P4-1/P4P5P4-1}$ .** Solutions of  $\text{P4M5P4-1}$  ( $2.5 \times 10^{-5}$  M) and  $\text{P4P5P4-1}$  ( $2.5 \times 10^{-5}$  M) in THF were prepared. The solutions of  $\text{P4M5P4-1}$  (0.5 mL) and  $\text{P4P5P4-1}$  (0.5 mL) were mixed in a volumetric flask (10 mL) at room temperature, to which trifluoromethylbenzene was added to make a solution (10 mL) of 10% THF/trifluoromethylbenzene with concentration of  $2.5 \times 10^{-6}$  M. This solution was diluted to  $2.5 \times 10^{-8}$  M, dropped on a freshly cleaved mica surface and dried in vacuo for AFM Analysis (Figure S10).

**Procedures for UV-vis Analyses of  $\text{P4P5P4-1/M4M5M4-1}$  in 10% THF/Trifluoromethylbenzene (Figure 25).** Solutions of  $\text{P4P5P4-1}$  ( $2.5 \times 10^{-5}$  M) and  $\text{M4M5M4-1}$  ( $2.5 \times 10^{-5}$  M) in THF were prepared. The solutions of  $\text{P4P5P4-1}$  (0.5 mL) and  $\text{M4M5M4-1}$  (0.5 mL) were mixed in a volumetric flask (10 mL) at room temperature, to which trifluoromethylbenzene was added to make a 10 mL solution. This solution was noted 10% THF/trifluoromethylbenzene with concentration of  $2.5 \times 10^{-6}$  M in this work. The UV-vis analyses were carried out at 25 °C.  $\text{P4M5P4-1/M4P5M4-1}$  was analyzed by the same procedures (Figure S18).

**Procedures for UV-vis Analyses of  $\text{P4P5P4-1/M4M5M4-1}$  in THF/Trifluoromethylbenzene/DMSO (Figure 28).** Solutions of  $\text{P4P5P4-1}$  ( $2.5 \times 10^{-5}$  M) and  $\text{M4M5M4-1}$  ( $2.5 \times 10^{-5}$  M) in THF were prepared. The solutions of  $\text{P4P5P4-1}$  (0.5 mL) and  $\text{M4M5M4-1}$  (0.5 mL) were mixed in a volumetric flask (10 mL) at room temperature, to which trifluoromethylbenzene was added to make a solution (10 mL) of 10% THF/trifluoromethylbenzene with concentration of  $2.5 \times 10^{-6}$  M. This solution (2 mL) was put in a quartz cell, and DMSO (0.06, 0.1, 0.2, and 0.4 mL) was added using microsyringe. The solutions were noted, in this work, 3%, 5%, 10%, and 20% DMSO content in 10% THF/trifluoromethylbenzene solution, respectively. The analyses were carried out at 25 °C.  $\text{P4M5P4-1/M4P5M4-1}$  was analyzed by the same procedures (Figure S21).

**Procedures for HPLC Measurements of  $\text{P4P5P4-1/M4M5M4-1}$  (Figure 26).** Solutions of  $\text{P4P5P4-1}$  ( $2.5 \times 10^{-5}$  M) and  $\text{M4M5M4-1}$  ( $2.5 \times 10^{-5}$  M) in THF were prepared. The solutions of  $\text{P4P5P4-1}$  (0.5 mL) and  $\text{M4M5M4-1}$  (0.5 mL) were mixed in a volumetric flask (10 mL) at room temperature, to which trifluoromethylbenzene was added to make a solution (10 mL) of 10% THF/trifluoromethylbenzene with concentration of  $2.5 \times 10^{-6}$  M. The measurement was carried out at room temperature.  $\text{P4M5P4-1/M4P5M4-1}$  was analyzed by the same procedures (Figure S19).

**Procedures for DLS Measurements of  $\text{P4P5P4-1/M4M5M4-1}$  (Figure 27).** Solutions of  $\text{P4P5P4-1}$  ( $5 \times 10^{-4}$  M) and  $\text{M4M5M4-1}$  ( $5 \times 10^{-4}$  M) in THF were prepared. The solutions of  $\text{P4P5P4-1}$  (0.1 mL) and  $\text{M4M5M4-1}$  (0.1 mL) were mixed in a grass vial at room temperature, to which trifluoromethylbenzene was added to make a solution (10 mL) of 10% THF/trifluoromethylbenzene with concentration of  $5 \times 10^{-5}$  M. The DLS measurements were carried out at 20 °C. Solvents were used after filtration through 0.2  $\mu\text{m}$  pore membrane filters.  $\text{P4M5P4-1/M4P5M4-1}$  was analyzed by the same procedures (Figure S20).

**Procedures for AFM Analyses of  $\text{P4P5P4-1/M4M5M4-1}$  (Figure S17).** Solutions of  $\text{P4P5P4-1}$  ( $2.5 \times 10^{-5}$  M) and  $\text{M4M5M4-1}$  ( $2.5 \times 10^{-5}$  M) in THF were prepared. The solutions of  $\text{P4P5P4-1}$  (0.5 mL) and  $\text{M4M5M4-1}$  (0.5 mL) were mixed in a volumetric flask (10 mL) at room temperature, to which trifluoromethylbenzene was added to make a solution (10 mL) of 10% THF/trifluoromethylbenzene with concentration of  $2.5 \times 10^{-6}$  M. This solution was diluted to  $2.5 \times 10^{-8}$  M, dropped on a freshly cleaved mica surface, and dried in vacuo for AFM analysis.  $\text{P4M5P4-1/M4P5M4-1}$  was analyzed by the same procedure (Figure S22).

**Procedures for CD and UV-vis Analyses of  $\text{P4P5P4-1/M4P5M4-1}$  (Figure S23).** Solutions of  $\text{P4P5P4-1}$  ( $2.5 \times 10^{-5}$  M) and  $\text{M4P5M4-1}$  ( $2.5 \times 10^{-5}$  M) in THF were prepared. The solutions of  $\text{P4P5P4-1}$  (0.5 mL) and  $\text{M4P5M4-1}$  (0.5 mL) were mixed in a volumetric flask (10 mL) at room temperature, to which trifluoromethylbenzene was added to make a solution (10 mL) of 10% THF/trifluoromethylbenzene with concentration of  $2.5 \times 10^{-6}$  M. The analyses were carried out at 25 °C.

**Procedures for HPLC Measurements of  $\text{P4P5P4-1/M4P5M4-1}$  (Figure S24).** Solutions of  $\text{P4P5P4-1}$  ( $2.5 \times 10^{-5}$  M) and  $\text{M4P5M4-1}$  ( $2.5 \times 10^{-5}$  M) in THF were prepared. The solutions of  $\text{P4P5P4-1}$  (0.5 mL) and  $\text{M4P5M4-1}$  (0.5 mL) were mixed in a volumetric flask (10 mL) at room temperature, to which trifluoromethylbenzene was added to make a solution (10 mL) of 10% THF/trifluoromethylbenzene with concentration of  $2.5 \times 10^{-6}$  M. The measurement was carried out at room temperature.

## ■ ASSOCIATED CONTENT

### 📄 Supporting Information

CD spectra of  $\text{P4M5P4-1}$  homoaggregates (Figures S1–S5) and  $\text{P4P5P4-1}$  aggregates (Figures S6 and S7), CD, UV-vis, AFM, and HPLC measurements of  $\text{P4M5P4-1/P4P5P4-1}$  heteroaggregates (Figures S8, S10–S16), UV-vis spectra of (*P*)-**4** (Figure S9), AFM analyses of racemic heteroaggregate  $\text{P4P5P4-1/M4M5M4-1}$  (Figure S17), UV-vis, HPLC, DLS, and AFM measurements of racemic heteroaggregates  $\text{P4M5P4-1/M4P5M4-1}$  (Figures S18–S22), CD, UV-vis, and HPLC measurements of  $\text{P4P5P4-1/M4P5M4-1}$  aggregates (Figures S23 and S24). This material is available free of charge via the Internet at <http://pubs.acs.org>.

## ■ AUTHOR INFORMATION

### Corresponding Author

\*E-mail: [yama@m.tohoku.ac.jp](mailto:yama@m.tohoku.ac.jp); fax: (+81) 22-795-6811.

### Notes

The authors declare no competing financial interest.

## ■ ACKNOWLEDGMENTS

We thank Professor Hiroyuki Isobe (Department of Chemistry, Graduate School of Sciences, Tohoku University) for allowing the use of DLS. This work was financially supported by a Grant-in-Aid for Scientific Research (No. 21229001). Financial support and a grant for research assistantship from the G-COE program from JSPS are also acknowledged. W. Ichinose thanks the JSPS for a Fellowship for Young Japanese Scientists.

## ■ REFERENCES

- (1) Petsko, A. G. *Protein Structure and Function*; New Science Press: London, United Kingdom, 2004.
- (2) (a) Niece, K. L.; Hartgerink, J. D.; Donners, J. J. J. M.; Stupp, S. I. *J. Am. Chem. Soc.* **2003**, *125*, 7146–7147. (b) Behanna, H. A.; Donners, J. J. J. M.; Gordon, A. C.; Stupp, S. I. *J. Am. Chem. Soc.* **2005**, *127*, 1193–1200. (c) Marsden, H. R.; Korobko, A. V.; Van Leeuwen, E. N. M.; Pouget, E. M.; Veen, S. J.; Sommerdijk, N. A. J. M.; Kros, A. *J. Am. Chem. Soc.* **2008**, *130*, 9386–9393.



(3) (a) Yang, X.; Hua, F.; Yamato, K.; Ruckenstein, E.; Gong, B.; Kim, W.; Ryu, C. Y. *Angew. Chem., Int. Ed.* **2004**, *43*, 6471–6474.

(b) Binder, W. H.; Kunz, M. J.; Kluger, C.; Hayn, G.; Saf, R. *Macromolecules* **2004**, *37*, 1749–1759.

(4) (a) Mather, B. D.; Baker, M. B.; Beyer, F. L.; Berg, M. A. G.; Green, M. D.; Long, T. E. *Macromolecules* **2007**, *40*, 6834–6845.

(b) McHale, R.; Patterson, J. P.; Zetterlund, P. B.; O'Reilly, R. K. *Nat. Chem.* **2012**, *4*, 491–497.

(5) (a) Tang, C.; Lennon, E. M.; Fredrickson, G. H.; Kramer, E. J.; Hawker, C. J. *Science* **2008**, *322*, 429–432. (b) Chen, W.-C.; Kuo, S.-W.; Lu, C.-H.; Jeng, U.-S.; Chang, F.-C. *Macromolecules* **2009**, *42*, 3580–3590. (c) Dobrosielska, K.; Takano, A.; Matsushita, Y. *Macromolecules* **2010**, *43*, 1101–1107.

(6) (a) Laffèche, F.; Durand, D.; Nicolai, T. *Macromolecules* **2003**, *36*, 1331–1340. (b) Nordskog, A.; Egger, H.; Findenegg, G. H.; Hellweg, T. *Phys. Rev. E* **2003**, *68*, 011406. (c) Dai, S.; Ravi, P.; Leong, C. Y.; Tam, K. C.; Gan, L. H. *Langmuir* **2004**, *20*, 1597–1604. (d) Kim, K. T.; Cornelissen, J. J. L. M.; Nolte, R. J. M.; Van Hest, J. C. M. *Adv. Mater.* **2009**, *21*, 2787–2791.

(7) (a) Lim, D. W.; Park, T. G. *J. Appl. Polym. Sci.* **2000**, *75*, 1615–1623. (b) Portinha, D.; Belleney, J.; Bouteiller, L.; Pensec, S.; Spassky, N. *Macromolecules* **2002**, *35*, 1484–1486. (c) Hiemstra, C.; Zhong, Z.; Li, L.; Dijkstra, P. J.; Feijen, J. *Biomacromolecules* **2006**, *7*, 2790–2795. (d) Wolf, F. K.; Hofmann, A. M.; Frey, H. *Macromolecules* **2010**, *43*, 3314–3324. (e) Nouailhas, H.; Ghzaoui, A. E.; Li, S.; Coudane, J. J. *Appl. Polym. Sci.* **2011**, *122*, 1599–1606.

(8) Examples of heteroaggregation by small organic molecules (self-sorting) are described in the following reviews: (a) Osowska, K.; Miljanić, O. Š. *Synlett* **2011**, *12*, 1643–1648. (b) Safont-Sempere, M. M.; Fernández, G.; Würthner, F. *Chem. Rev.* **2011**, *111*, 5784–5814. (c) Chakrabaty, R.; Mukherjee, P. S.; Stang, P. J. *Chem. Rev.* **2011**, *111*, 6810–6918. (d) Lal Saha, M.; Schmittel, M. *Org. Biomol. Chem.* **2012**, *10*, 4651–4684.

(9) Ichinose, W.; Shigeno, M.; Yamaguchi, M. *Chem.—Eur. J.* **2012**, *18*, 12644–12654.

(10) Amemiya, R.; Ichinose, W.; Yamaguchi, M. *Bull. Chem. Soc. Jpn.* **2010**, *83*, 809–815.

(11) (a) Sugiura, H.; Nigorikawa, Y.; Saiki, Y.; Nakamura, K.; Yamaguchi, M. *J. Am. Chem. Soc.* **2004**, *126*, 14858–14864. (b) Sugiura, H.; Yamaguchi, M. *Chem. Lett.* **2007**, *36*, 58–59. (c) Sugiura, H.; Amemiya, R.; Yamaguchi, M. *Chem. Asian J.* **2008**, *3*, 244–260. (d) Amemiya, R.; Saito, N.; Yamaguchi, M. *J. Org. Chem.* **2008**, *73*, 7137–7144. (e) Amemiya, R.; Yamaguchi, M. *Org. Biomol. Chem.* **2008**, *26*–35. (f) Saito, N.; Terakawa, R.; Shigeno, M.; Amemiya, R.; Yamaguchi, M. *J. Org. Chem.* **2011**, *76*, 4841–4858. (g) Yamamoto, K.; Sugiura, H.; Amemiya, R.; Aikawa, H.; An, Z.; Yamaguchi, M.; Mizukami, M.; Kurihara, K. *Tetrahedron* **2011**, *67*, 5972–5978.

(12) Saito, N.; Shigeno, M.; Yamaguchi, M. *Chem.—Eur. J.* **2012**, *18*, 8994–9004.

(13) (a) Mizutani, M.; Amemiya, R.; Yamaguchi, M. *Angew. Chem., Int. Ed.* **2010**, *49*, 1995–1999. (b) Yamamoto, K.; Oyamada, N.; Mizutani, M.; An, Z.; Saito, N.; Yamaguchi, M.; Kasuya, M.; Kurihara, K. *Langmuir* **2012**, *28*, 11939–11947.

(14) See following for heteroaggregation of double stranded organic molecules (a) Zhan, C.; Léger, J.-M.; Huc, I. *Angew. Chem., Int. Ed.* **2006**, *45*, 4625–4628. (b) Goto, H.; Furusho, Y.; Yashima, E. *J. Am. Chem. Soc.* **2007**, *129*, 9168–9174. (c) Ito, H.; Furusho, Y.; Hasegawa, T.; Yashima, E. *J. Am. Chem. Soc.* **2008**, *130*, 14008–14015. (d) Gan, Q.; Li, F.; Li, G.; Kauffmann, B.; Xiang, J.; Huc, I.; Jiang, H. *Chem. Commun.* **2010**, *46*, 297–299. (e) Wang, H.-B.; Mudraboyina, B. P.; Wisner, J. A. *Chem.—Eur. J.* **2012**, *18*, 1322–1327.